THE JOURNAL OF BIOLOGICAL CHEMISTRY VOL. 281, NO. 20, pp. 14192–14206, May 19, 2006

Alkylamides from *Echinacea* Are a New Class of Cannabinomimetics

CANNABINOID TYPE 2 RECEPTOR-DEPENDENT AND -INDEPENDENT IMMUNOMODULATORY EFFECTS[*][S]

Received for publication, February 3, 2006, and in revised form, March 13, 2006 Published, JBC Papers in Press, March 17, 2006, DOI 10.1074/jbc.M601074200

Stefan Raduner[‡], Adriana Majewska[‡], Jian-Zhong Chen[§], Xiang-Qun Xie[§], Jacques Hamon[¶], Bernard Faller[¶], Karl-Heinz Altmann[‡], and Jürg Gertsch[‡1]

From the [‡]Department of Chemistry and Applied Biosciences, ETH Zurich, Wolfgang-Pauli-Strasse 10, CH-8093 Zürich, Switzerland, the [§]Department of Pharmacological and Pharmaceutical Sciences, College of Pharmacy, University of Houston, Houston, Texas 77204-5037, and [¶]Novartis Institutes for BioMedical Research, Discovery Technologies, 4002 Basel, Switzerland

Alkylamides (alkamides) from *Echinacea* modulate tumor necrosis factor α mRNA expression in human monocytes/macrophages via the cannabinoid type 2 (CB_2) receptor (Gertsch, J., Schoop, R., Kuenzle, U., and Suter, A. (2004) *FEBS Lett.* 577, 563–569). Here we show that the alkylamides dodeca-2*E*,4*E*,8*Z*,10*Z*-tetraenoic acid isobutylamide (A1) and dodeca-2*E*,4*E*-dienoic acid isobutylamide (A2) bind to the CB_2 receptor more strongly than the endogenous cannabinoids. The K_i values of A1 and A2 (CB_2 ~60 nM; CB_1 >1500 nM) were determined by displacement of the synthetic high affinity cannabinoid ligand [^{3}H]CP-55,940. Molecular modeling suggests that alkylamides bind in the solvent-accessible cavity in CB_2, directed by H-bonding and π-π interactions. In a screen with 49 other pharmacologically relevant receptors, it could be shown that A1 and A2 specifically bind to CB_2 and CB_1. A1 and A2 elevated total intracellular Ca^{2+} in CB_2-positive but not in CB_2-negative promyelocytic HL60 cells, an effect that was inhibited by the CB_2 antagonist SR144528. At 50 nM, A1, A2, and the endogenous cannabinoid anandamide (CB_2 K_i >200 nM) up-regulated constitutive interleukin (IL)-6 expression in human whole blood in a seemingly CB_2-dependent manner. A1, A2, anandamide, the CB_2 antagonist SR144528 (K_i <10 nM), and also the non-CB_2-binding alkylamide undeca-2*E*-ene,8,10-diynoic acid isobutylamide all significantly inhibited lipopolysaccharide-induced tumor necrosis factor α, IL-1β, and IL-12p70 expression (5–500 nM) in a CB_2-independent manner. Alkylamides and anandamide also showed weak differential effects on anti-CD3- *versus* anti-CD28-stimulated cytokine expression in human whole blood. Overall, alkylamides, anandamide, and SR144528 potently inhibited lipopolysaccharide-induced inflammation in human whole blood and exerted modulatory effects on cytokine expression, but these effects are not exclusively related to CB_2 binding.

Purple coneflower (*Echinacea purpurea* and *Echinacea angustifolia*) preparations are widely used herbal medicines for the treatment of the common cold and upper respiratory infections (1, 2). It is generally believed that *Echinacea* affords its benefits through interactions with the immune system (3), but data on the clinical efficacy of *Echinacea* in the treatment of the common cold and upper respiratory infections are contradictory (4, 5). In contrast to the significant investments into the clinical assessment of the efficacy of *Echinacea* (6), the molecular mechanism of action of this medicinal plant has remained elusive, and comprehensive studies on the immunomodulatory actions of *Echinacea* constituents are scarce.

We have reported previously that unsaturated fatty acid *N*-alkylamides (alkylamides) from *Echinacea* preparations can modulate the expression of TNF-α[2] in human monocytes and macrophages (Mϕs) *in vitro* (7). We ascribed these effects to interactions of alkylamides with the cannabinoid type 2 receptor (CB_2) on monocytes, resulting in the activation of c-Jun N-terminal kinase, mitogen-activated protein kinase, and of the nuclear factor κB (NF-κB), which ultimately leads to TNF-α mRNA expression (7). In the same study it was demonstrated that alkylamides inhibit LPS-stimulated TNF-α protein expression from isolated monocytes/Mϕs. These findings were independently confirmed in a more recent study, which demonstrated binding of alkylamides from *E. angustifolia* to rodent cannabinoid receptors and inhibition of fatty acid amide hydrolase, the enzyme that controls the half-life of the endogenous cannabinoid ligand anandamide (8).

Cannabinoid receptors belong to the G-protein-coupled receptor (GPCR) family and are ubiquitously found in the central nervous system and in the periphery. So far, two types of receptors have been characterized, which are referred to as type 1 (CB_1) and type 2 (CB_2) receptors. The CB_1 receptor is predominantly but not exclusively found in the nervous system, whereas the CB_2 receptor is mainly expressed on immune cells and in the spleen (9, 10).

Because of its role in the cellular immune system, the CB_2 receptor is of particular interest for our ongoing studies on the immunomodulatory activity of alkylamides from *Echinacea*. In fact, the CB_2 receptor is abundantly expressed in different types of inflammatory and immune-competent cells (11, 12), and there is accumulating evidence that the CB_2 receptor plays a role in inflammatory reactions and the immune response (13–15), as well as related pathophysiological conditions (16, 17). It is also well established that cannabinoids mediate both inhibitory and stimulatory effects on the immune system by modulating cytokine expression (18, 19). These differential effects are also dependent on

* The costs of publication of this article were defrayed in part by the payment of page charges. This article must therefore be hereby marked "*advertisement*" in accordance with 18 U.S.C. Section 1734 solely to indicate this fact.

[S] The on-line version of this article (available at http://www.jbc.org) contains supplemental Figs. 1 and 2.

[1] To whom correspondence should be addressed. Tel.: 41-44-633-7374; Fax: 41-44-633-1366; E-mail: juerg.gertsch@pharma.ethz.ch.

[2] The abbreviations used are: TNF-α, tumor necrosis factor α; 2-AG, 2-arachidonoyl-glycerol; CB, cannabinoid receptor; FACS, fluorescence-activated cell sorting; GM-CSF, granulocyte colony-stimulating factor; GPCR, G-protein-coupled receptor; LPS, lipopolysaccharide; NF-κB, nuclear factor κB; IL, interleukin; Mϕs, macrophages; PLC, phospholipase C; PMA, phorbol ester (12-tetradecanoylphorbol-13 acetate); BisTris, 2-[bis(2-hydroxyethyl)-amino]-2-(hydroxymethyl)propane-1,3-diol; A1, dodeca-2*E*,4*E*,8*Z*,10*Z*-tetraenoic acid isobutylamide; A2, dodeca-2*E*,4*E*-dienoic acid isobutylamide; A3, undeca-2*E*-ene,8,10-diynoic acid isobutylamide; CBA, cytometric bead array.

ligand concentration (19), but the underlying mechanisms of the concentration effects are not yet understood. Recent studies also highlight the potential of CB_2 receptor ligands in the treatment of cancer (20, 21) and atherosclerosis (22).

Therefore, the general aim of this study was to characterize the interaction of alkylamides from the medicinal plant *Echinacea* with the human CB_2 receptor with respect to binding affinity, ligand specificity, and functional consequences at physiological drug concentrations in cellular systems *in vitro*. Binding studies were based on radioligand displacement assays with the bicyclic cannabinoid ligand [^{3}H]CP-55,940, which has played an important role in the discovery of the cannabinoid receptors (23, 24), and which strongly binds to the cannabinoid-binding site in CB_2 (K_i = 0.7 nM). Despite the fact that more than one plausible binding site in CB_2 has been postulated (25), the CP-55,940-binding site is shared by all cannabinoids reported so far. The experimental investigations were complemented by molecular modeling studies based on a previously established homology model (25). No experimental information is currently available on the structure of the receptor.

We have shown previously that alkylamides inhibit forskolin-induced cAMP production (7) via the CB_2 receptor. To further characterize the direct functional effects of alkylamide binding to the CB_2 receptor, the total intracellular free Ca^{2+} concentration ($[Ca^{2+}]_i$) in both CB_2-expressing (CB_2-positive) and CB_2-nonexpressing (CB_2-negative) HL60 cells was measured. In addition to defined cellular systems, we have also investigated the effects of nanomolar concentrations of alkylamides on cytokine expression in human peripheral whole blood cultures, both under nonstimulating and stimulating conditions. Immunomodulatory actions of endogenous and exogenous cannabinoids have been investigated in numerous studies (18), mostly performed with isolated cells or transformed cell lines, but only sparse data exist for *ex vivo* studies or studies with whole blood. Recent reports have shown that plasma levels of alkylamides in the lower nanomolar range can be achieved in humans after oral administration of commercial alkylamide-containing *Echinacea* preparations (26, 27). So far, however, it is not known whether alkylamides can exert immunomodulatory effects via the CB_2 receptor at such low concentrations. Whole blood rather than isolated leukocytes were chosen for these studies in order to simulate physiological conditions as closely as possible. Whole blood studies were performed with three major alkylamides from *Echinacea*, the endogenous cannabinoid arachidonoylethanolamide (anandamide), and the CB_2 antagonist SR144528 (28).

EXPERIMENTAL PROCEDURES

Cell Culture—Human promyelocytic leukemia non-CB_2-expressing (negative) HL60 cells (obtained from Prof. Dr. Verena Dirsch, Vienna, Austria) were grown in RPMI 1640 medium (Invitrogen) supplemented with 10% fetal bovine serum, 1 g/ml fungizone (amphotericin B), 100 units/ml penicillin, 100 g/ml streptomycin, and 2 mM L-glutamine (all from Invitrogen). Human promyelocytic leukemia CB_2-expressing (positive) HL60 cells (obtained from the ATCC, CCL-240) were grown in Iscove's modified Dulbecco's medium with 4 mM L-glutamine and 1.5 g/liter sodium bicarbonate (ATCC, Manassas, VA) supplemented with 20% fetal bovine serum, 1 g/ml fungizone (amphotericin B), 100 units/ml penicillin, and 100 g/ml streptomycin. The human CB_2-expressing CHO-K1 cells were grown in the same medium as the CB_2-negative HL60 cells but supplemented with 400 μg/ml G418 (10131-027; Invitrogen). All cells were grown in a humidified incubator at 37 °C and 5% CO_2.

Human Peripheral Whole Blood Cultures—10 ml of peripheral whole blood was obtained from healthy volunteers in the early afternoon by a medical doctor. The blood was collected into heparinized tubes (BD Vacutainer Systems) and gently shaken for 1 min. 200-μl portions were then immediately aliquoted into a 96-well plate under sterile conditions. Each experiment was carried out in triplicate. Test compounds and vehicle controls were added. After 45 min of incubation in a humidified incubator at 37 °C and 5% CO_2, stimulation of cells was initiated by addition of either 313 ng/ml LPS, 1 μg/ml αCD3 (combined with 1.5 μg/ml PMA), or 0.5 μg/ml αCD28 (combined with 1.5 μg/ml PMA) to the blood culture under gentle stirring. Volumes of stimulatory mixtures were set to 2 μl. PMA stimulation alone did not markedly induce cytokines in whole blood. Again, vehicle controls (ethanol or H_2O) of the same dilutions were included. The plate was then incubated at 37 °C and 5% CO_2 for 18 h. After incubation the plates were centrifuged at room temperature for 5 min at 450 rpm in an MSE Mistral 3000i centrifuge to facilitate plasma collection. For each assay at least three experiments were performed in triplicate with blood from at least three different donors (total of at least nine measurements).

FACS Analysis of CB_2 Expression—HL60 or CB_2-transfected CHO-K1 cells (10^6) were washed in phosphate-buffered saline (Invitrogen) supplemented with 0.1% NaN_3 and 2% fetal bovine serum and incubated (1:100) with the rabbit polyclonal CB_2-specific antibody (3561) for 45 min on ice in the dark. After two washing steps, the cells were incubated (1:32) with a monoclonal anti-rabbit fluorescein isothiocyanate-labeled antibody for 45 min on ice in the dark. The cells were washed twice and resuspended in 500 μl of phosphate-buffered saline with 0.1% NaN_3 and 1% *p*-formaldehyde prior to analysis on a FACScan cytometer (BD Biosciences). Measurements were carried out with the CellQuest™ software, and relative expressions were compared with secondary antibody controls.

Radioligand Displacement Assays on CB_1 and CB_2 Receptors—For the CB_1 receptor, binding experiments were performed in the presence of 0.39 nM of the radioligand [^{3}H]CP-55,940 at 30 °C in siliconized glass vials together with 7.16 μg of membrane recombinantly overexpressing CB_1 (RBHCB1M; PerkinElmer Life Sciences), which was resuspended in 0.2 ml (final volume) of binding buffer (50 mM Tris-HCl, 2.5 mM EGTA, 5 mM $MgCl_2$, 0.5 mg/ml fatty acid free bovine serum albumin, pH 7.4). Test compounds were present at varying concentrations, and the nonspecific binding of the radioligand was determined in the presence of 10 μM CP-55,940. After 90 min of incubation, the suspension was rapidly filtered through 0.05% polyethyleneimine pre-soaked GF/C glass fiber filters on a 96-well cell harvester and washed nine times with 0.5 ml of ice-cold washing buffer (50 mM Tris-HCl, 2.5 mM EGTA, 5 mM $MgCl_2$, 2% bovine serum albumin, pH 7.4). Radioactivity on filters was measured with a Beckman LS 6500 scintillation counter in 3 ml of Ultima Gold scintillation liquid. Data collected from three independent experiments performed in triplicate were normalized between 100 and 0% specific binding for [^{3}H]CP-55,940. These data were graphically linearized by projecting Hill plots, which allowed the calculation of IC_{50} values. Derived from the dissociation constant (K_D) of [^{3}H]CP-55,940 and the concentration-dependent displacement (IC_{50} value), inhibition constants (K_i) of competitor compounds were calculated using the Cheng-Prusoff equation ($K_i = IC_{50}/(1 + L/K_D)$) (29).

For CB_2 receptor binding studies, 3.8 μg of membrane recombinantly overexpressing CB_2 (RBXCB2M; PerkinElmer Life Sciences) was resuspended in 0.6 ml of binding buffer (see above) together with 0.11 nM of the radioligand [^{3}H]CP-55,940. The CB_2-binding assay was conducted in the same manner as for CB_1.

Western Blotting—HL60 cells and CB_2-transfected CHO-K1 cells were resuspended and homogenized in ice-cold buffer A (15 mM Tris-HCl, 2 mM $MgCl_2$, 0.3 mM EDTA, 1 mM EGTA, pH 7.5) followed by

centrifugation at 40,000 × *g* for 25 min at 4 °C. The pellet was washed with buffer A and centrifuged again at 40,000 × *g* for 25 min at 4 °C. The membrane was resuspended in buffer B (75 mM Tris-HCl, 12.5 mM $MgCl_2$, 0.3 mM EDTA, 1 mM EGTA, 250 mM sucrose, pH 7.5) and stored at −80 °C until used. All membrane preparation steps were performed in the presence of protease inhibitor mixture (P8340; Sigma).

Membrane proteins were separated on 4–12% Nupage™ Novex BisTris pre-cast gels (Invitrogen) under denaturing and nonreducing conditions and subsequently transferred to nitrocellulose membranes. Blocking of membrane, incubation of the primary and secondary antibodies, and detection by chemiluminescence following ECL Plus Western blotting Detection Reagents (Amersham Biosciences) were performed according to the manufacturer's instructions.

Receptor Screen—The receptor screen was carried out at the Novartis Institute for Biomedical Research in Basel, Switzerland. 10 μM of test compound was subjected to cell membrane preparations from cell lines overexpressing specific receptors in order to test for competitive binding with the corresponding radioligands. Inhibitions of >50% were significantly higher than background interference and represent specific positive interactions with the radioligand-binding sites.

CB_2 Homology Model and Docking Study—The program HOMOLOGY/InsightII (MSI-Biosym InsightII/Homology version 98, MSI Inc., San Diego) was used to generate the initial three-dimensional structural model of the CB_2 receptor based on the x-ray crystal structure of bovine rhodopsin (30). Multiple sequence alignment among 10 selective GPCRs, including the CB_2 receptor and bovine rhodopsin from the rhodopsin GPCR family, was first performed to distinguish the seven transmembrane domains and extra- and intra-loop regions of the receptors, and the results were refined and evaluated by mutation scores, pairwise hydrophobicity profiles, and Kyte-Doolittle plots. The CB_2 three-dimensional structural model was then constructed by mapping the CB_2 sequence on the homologous residues of the rhodopsin x-ray structure in 7TM regions and searching for homologous C-α backbone sequences in published structures from the Protein Data Bank in loop regions. The energy minimization and molecular dynamics (MD/MM) simulation was finally carried out to optimize the CB_2 three-dimensional structural model (25). To explore the possible binding pocket or domain(s) inside the CB_2 receptor, molecular surface and physicochemical property maps, *i.e.* electrostatic and hydrophobicity (lipophilicity) potentials, were generated on the Connolly solvent-accessible surface by using the MOLCAD program (SYBYL7.0) (molecular modeling software packages, version 7.0, Tripos Associates, Inc., St. Louis). MOLCAD's rendering techniques allow the rapid calculation and display of property-coded surfaces for the molecular recognition. The generated surface property maps were further examined for the complementary biological data.

The alkylamide docking and CB_2 protein-ligand complex studies were performed on the basis of the following docking protocol by using Tripos molecular modeling packages Sybyl7.0 on an SGI octane computer. First, a three-dimensional structure of the alkylamide molecule was built by the Sketch module in Sybyl7.0 and optimized by using the Tripos force field. The initial docking position of alkylamide molecules was established inside the hypothetic binding pocket that was defined on the basis of the MOLCAD-generated solvent-accessible cavity model of the CB_2 receptor. Then the receptor-ligand binding geometry was optimized by flexible docking using the FlexiDock module in Sybyl7.0. During flexible docking simulation, the single bonds of the alkylamide and all side chains within the defined binding region, or 3 Å around the target ligand, of the CB_2 receptor were defined as rotatable or flexible bonds, and the ligand was allowed to move flexibly within the tentative binding site/pocket. The atomic charges were recalculated by using Kollman all-atom for the protein and Gasteiger-Hückel for the ligand. The interaction energy was calculated using van der Waals, electrostatic, and torsional energy terms of the Tripos force field. The iterations were set at 20,000 generations for genetic algorithms.

Subsequently, further optimization was carried out on the FlexiDock-generated CB_2 receptor-ligand complexes by using energy minimization and molecular dynamics. In this study, the AMBER force field along with a 15-Å cut-off distance for nonbonded interactions was applied to optimize the intermediate ligand-bound CB_2 receptor model. A distance-dependent ($\varepsilon = 5r$) dielectric function was used. Before the optimization, a binding pocket was defined to include the ligand and the residues within 7.5 Å around the ligand in the complex. The molecular dynamics protocol consisted of the following. (i) Initial minimization for 500 iterations of steepest descents, followed by conjugate gradients minimization, until the root mean square deviation became less than 0.1 $kcal \cdot mol^{-1} \cdot Å^{-1}$. (ii) MD simulations were then performed at a constant temperature of 1000 K and a time step of 1 fs for a total of 50 ps. Initially, a constraint was applied to keep the backbone atoms in the seven transmembrane domains inside the binding pocket and all of other atoms outside the binding pocket of the CB_2 receptor. Fifty representative snapshots of the ligand receptor complex from the molecular dynamics run were retrieved, minimized with 500 iterations of steepest descent, and followed by conjugate gradient minimization until the maximum derivative was less than 0.1 $kcal \cdot mol^{-1} \cdot Å^{-1}$. The minimization and molecular dynamics simulation of the ligand receptor complex were further analyzed and evaluated as described later.

Measurement of $[Ca^{2+}]_i$—HL60 CB_2-positive cells were washed once, and cells (10^7 cells/ml) were incubated at 37 °C for 20 min in Hanks' balanced salt solution containing fluo3/AM in a final concentration of 4 μM and 0.15 mg/ml Pluronic F-127. The cells were then diluted 1:5 in Hanks' balanced salt solution containing 1% fetal bovine serum and incubated for 40 min at 37 °C. Afterward, the cells were washed three times and resuspended in 500 μl of Ca^{2+}-free HEPES-buffered saline, containing 137 mM NaCl, 5 mM KCl, 1 mM Na_2HPO_4, 5 mM glucose, 0.5 mM $MgCl_2$, 0.1 mM EGTA, 1 g/liter bovine serum albumin, 10 mM Hepes, pH 7.4. Prior to each measurement, the cells were incubated for 7 min in a 37 °C water bath. In some experiments the cells were pretreated for 4 min with SR144528 (1 μM). The cells were subsequently stimulated with drugs and vehicle controls and analyzed with the FL1 channel on a FACScan flow cytometer equipped with a 488 nm argon laser (BD Biosciences). Because the solvent (ethanol) showed an effect on $[Ca^{2+}]_i$ in vehicle controls, this solvent effect was subtracted from each value.

Quantification of Cytokines with CBAs—Cytokine production in human peripheral whole blood was analyzed in blood plasma or supernatants of cells cultured for 18 h at 37 °C, 5% CO_2 using Cytometric Bead Arrays™ (BD Biosciences). Blood cultures were carried out as described above. IL-12p70, TNF-α, IL-10, IL-6, IL-1β, and IL-8 were detected using the human inflammation CBA kit (551811; BD Biosciences), and for GM-CSF, IL-7, IL-5, IL-4, and IL-3 detection the human allergy CBA kit (558022; BD Biosciences) was used. Tests were performed according to the manufacturer's instructions. Briefly, 50 μl of supernatants were mixed with 50 μl of phycoerythrin-conjugated cytokine capture beads. For each set of experiments a standard curve was generated. Prior to each measurement the red and orange channels were adequately compensated, according to instructions. FL-2 was typically compensated for 40% FL-1. After 3 h of incubation, samples were rinsed, fixed with 1% paraformaldehyde, and analyzed by flow cytometry (FACScan and

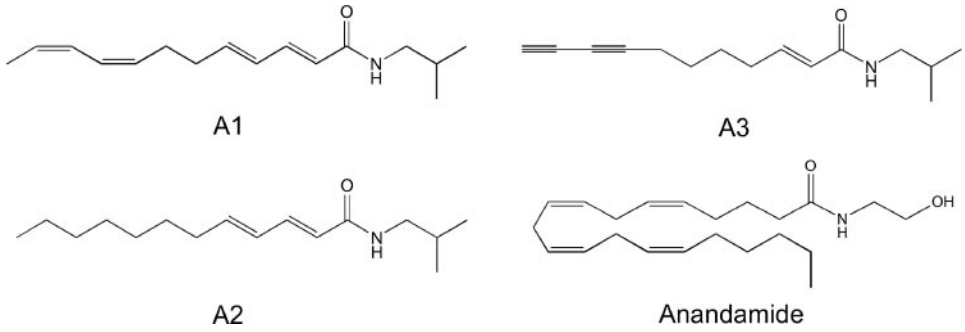

FIGURE 1. **Molecular structures of alkylamides and anandamide.**

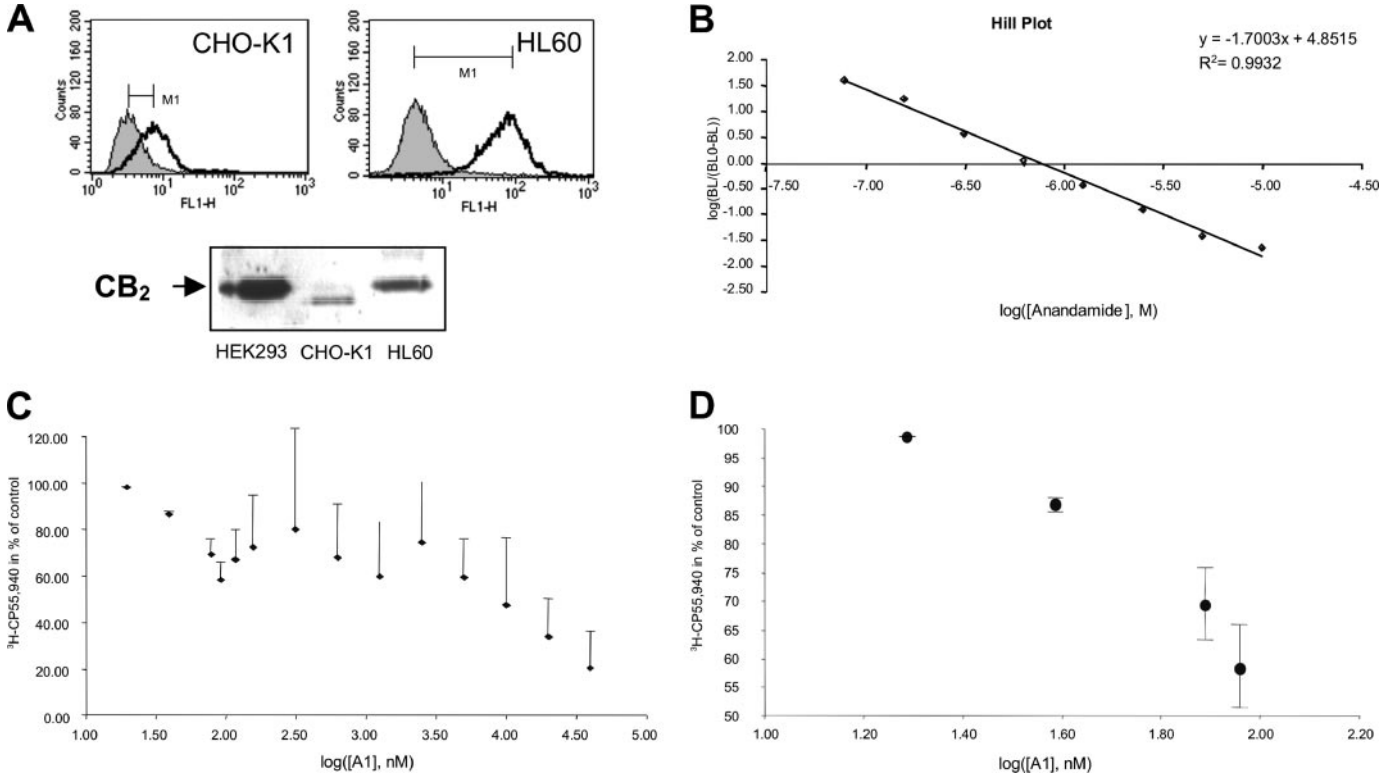

FIGURE 2. **Cellular CB_2 expression and [^{3}H]CP-55,940 displacement from human CB_2 receptor.** *A,* expression of the CB_2 receptor on HEK293 cells (RBXCB2M; PerkinElmer Life Sciences), CB_2-transfected CHO-K1 cells, and CB_2-positive promyelocytic HL60 cells (CCL-240; ATCC) as determined by semiquantitative Western blotting and FACS. *B,* Hill plot showing displacement of [^{3}H]CP-55,940 by anandamide. *C,* displacement of [^{3}H]CP-55,940 by A1 showing a biphasic curve ($n = 4 \pm$ S.D.). *D,* low concentration part of displacement curve by A1 ($n = 4 \pm$ S.D.).

FACSCanto) with the CBA Analysis Software; BD Biosciences). The results were expressed as pg/ml and then analyzed for their relative expression (control *versus* treated sample). The lower limit of detection for each cytokine was determined as 20 pg/ml.

Drugs and Antibodies—Dodeca-2*E*,4*E*-dienoic acid isobutylamide (A2) was isolated from *E. purpurea* as published previously (31) for *E. angustifolia* root material. Dodeca-2*E*,4*E*,8*Z*,10*Z*-tetraenoic acid isobutylamide (A1) and undeca-2*E*-en-8,10-diynoic acid isobutylamide (A3) were gifts from R. Lehmann (MediHerb, Australia). Compounds were checked for identity and integrity by thin layer chromatography and ^{1}H NMR (500 MHz Bruker) spectroscopy prior to use. Anandamide, 2-AG, AM630, and CP-55,940 were obtained from Tocris Cookson Ltd. (UK). SR144528 was obtained as a gift from Sanofi-Synthélabo Recherche (France). Fluo3/AM, Pluronic F-127, and the monoclonal anti-rabbit fluorescein isothiocyanate antibody were purchased from Sigma. CB_2 rabbit polyclonal antibody (3561) was obtained from Abcam (UK) and was tested for differential binding to immune cells. The radioligand [^{3}H]CP-55,940 was obtained from PerkinElmer Life Sciences. Anandamide, LPS (*E. coli*, serotype 055:B5), and PMA (from Euphorbiaceae) were obtained from Fluka Chemie, Switzerland. Thapsigargin was purchased from Alexis Biochemicals, Switzerland. Monoclonal αCD3 (555336) and αCD28 (348040) were purchased from Pharmingen.

Calculations and Statistics—Results are expressed as mean values ± S.D. or ± S.E. for each examined group. Statistical significance of differences between groups was determined by the Student's *t* test (paired *t* test) with GraphPad Prism software. Outliners in a series of identical experiments were determined by Grubb's test (ESD method) with α set to 0.05. Statistical differences between treated and vehicle control groups were determined by Student's *t* test for dependent samples. Differences between the analyzed samples were considered as significant if $p \leq 0.05$.

RESULTS

The solubility of the lipophilic alkylamides A1 and A2 is limited in aqueous solutions as detected by a Tyndall effect at concentrations

above 10 μM, and even low alkylamide concentrations (~300 nM) resulted in the formation of detectable particles in buffer (not shown). For the interpretation of the results obtained in the biological assays, it is therefore important to consider the possibility that the actual free alkylamide concentration in the culture medium may be less than the calculated nominal concentration.

Binding Studies—To determine whether alkylamides A1, A2, and A3 (Fig. 1) bind to the human CB_2 receptor as proposed previously (7), we first evaluated different CB_2 receptor expression systems by Western blotting and fluorescence-activated cytometry, using a polyclonal human CB_2 antibody (3560). The human CB_2 receptor recombinantly expressed in CHO-K1 cells and naturally expressed on original human promyelocytic HL60 cells (ATCC No CCL-240) was clearly detectable (Fig. 2*A*). However, CB_2-transfected HEK293 cells (RBXCB2M; PerkinElmer Life Sciences) showed the strongest CB_2 expression with a receptor glycosylation status comparable with the one found in HL60 cells as judged by the band size on Western blots (Fig. 2*A*). Based on the results from [^{3}H]CP-55,940 displacement with anandamide (low non-specific binding), which was used as positive control (Fig. 2*B*), we selected membrane preparations obtained from CB_2 and CB_1 overexpressing HEK293 cells, respectively, for all subsequent experiments (see "Experimental Procedures"). Cichoric acid, which is another prominent constituent in *Echinacea,* and arachidonic acid were included as negative controls in the binding studies.

TABLE 1
K_i values of compounds tested
$n = 3 \pm$ S.D.

Compound	K_i of human CB_2	K_i of human CB_1
	nM	
A1	57 ± 14	6210 ± 800
A2	60 ± 13	1940 ± 370
A3	>40,000	>40,000
Δ^9-Tetrahydrocannabinol	36.4 ± 10[a]	40.7 ± 2[a]
Anandamide	218 ± 149	37
2-AG	1400[b]	472[b]
Arachidonic acid	>40,000	>40,000
Cichoric acid	>40,000	ND[c]
SR144528	0.6[d]	437[d]

[a] See Ref. 63.
[b] See Ref. 64.
[c] ND indicates not determined.
[d] See Ref. 65.

Anandamide showed a concentration-dependent displacement of the radioligand [^{3}H]CP-55,940 from membrane preparations with a determined K_i of 218 ± 149 nM (Fig. 2*B*). At concentrations below 100 nM, alkylamides A1 and A2 potently displaced the radioligand in a concentration-dependent manner, but the displacement curve showed a second phase at higher ligand concentrations (Fig. 2*C*), which may reflect solubility problems and the formation of alkylamide particles. Based on the low concentration part of the displacement curve (Fig. 2*D*), A1 and A2 showed high affinity toward CB_2 with K_i values of 57 ± 14 nM (A1) and 60 ± 13 nM (A2). Significantly lower affinity was observed toward CB_1 (Table 1). Cichoric acid, arachidonic acid, and the alkylamide A3 did not displace [^{3}H]CP-55,940 (K_i > 40,000 nM) from CB_2 (Table 1) and therefore do not bind to the cannabinoid-binding site.

Receptor Screen—To assess the specificity of the binding to cannabinoid receptors relative to other potential targets, A1 and A2 (10 μM each) were subjected to a receptor screen (see "Experimental Procedures"). The screen included CB_1 and 49 additional pharmaceutically

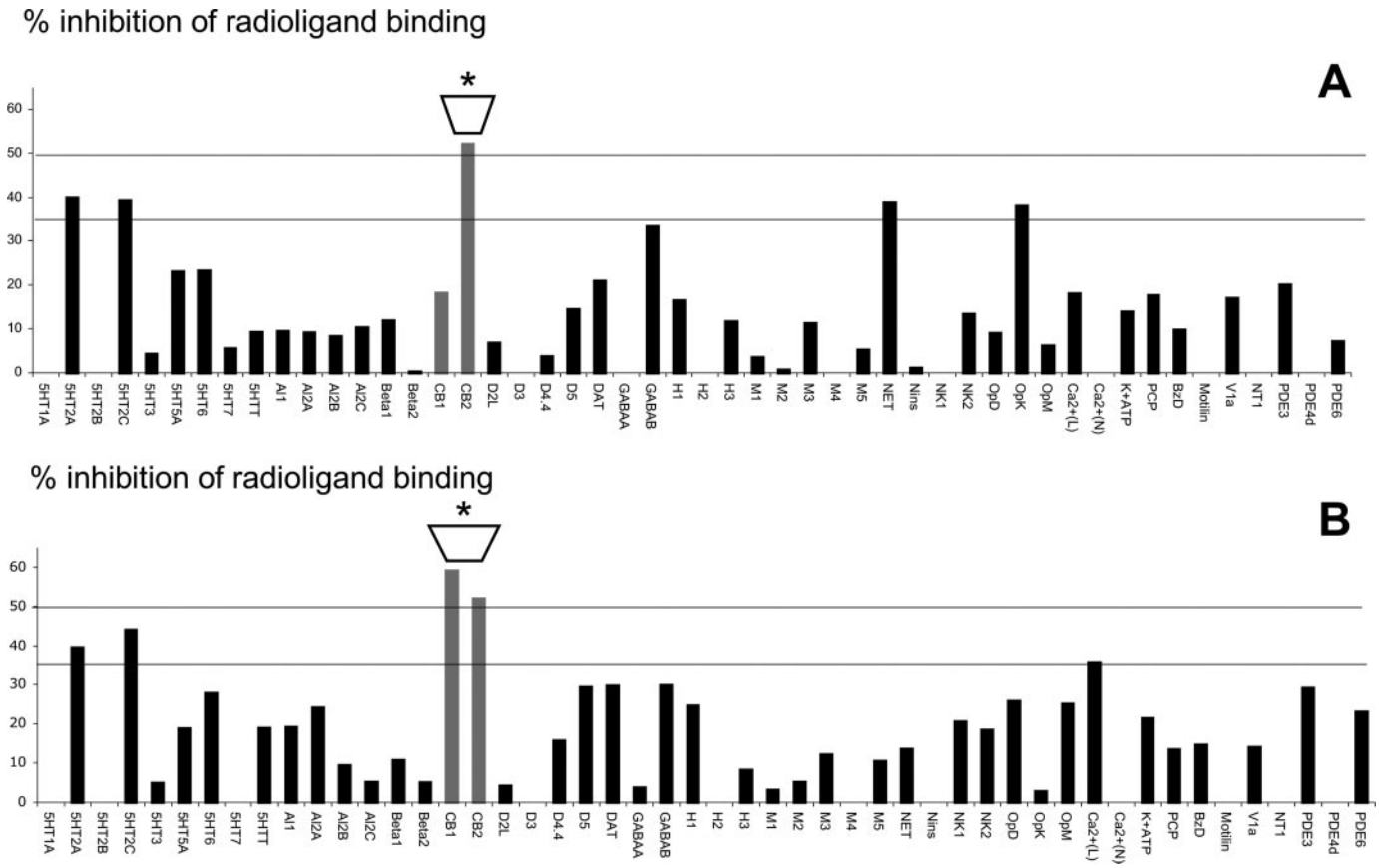

FIGURE 3. **Alkylamides A1 and A2 specifically bind to cannabinoid receptors.** A1 and A2 (10 μM each) were subjected to a receptor screen. The alkylamide A1 significantly inhibits (>50%) radioligand binding to CB_2 (*A*); the alkylamide A2 significantly inhibits (>50%) radioligand binding to CB_1 and CB_2 (*B*). Data are from single measurements. In this test system, the probability that a test compound inhibits binding of radioligands by 50% by chance is <5%.

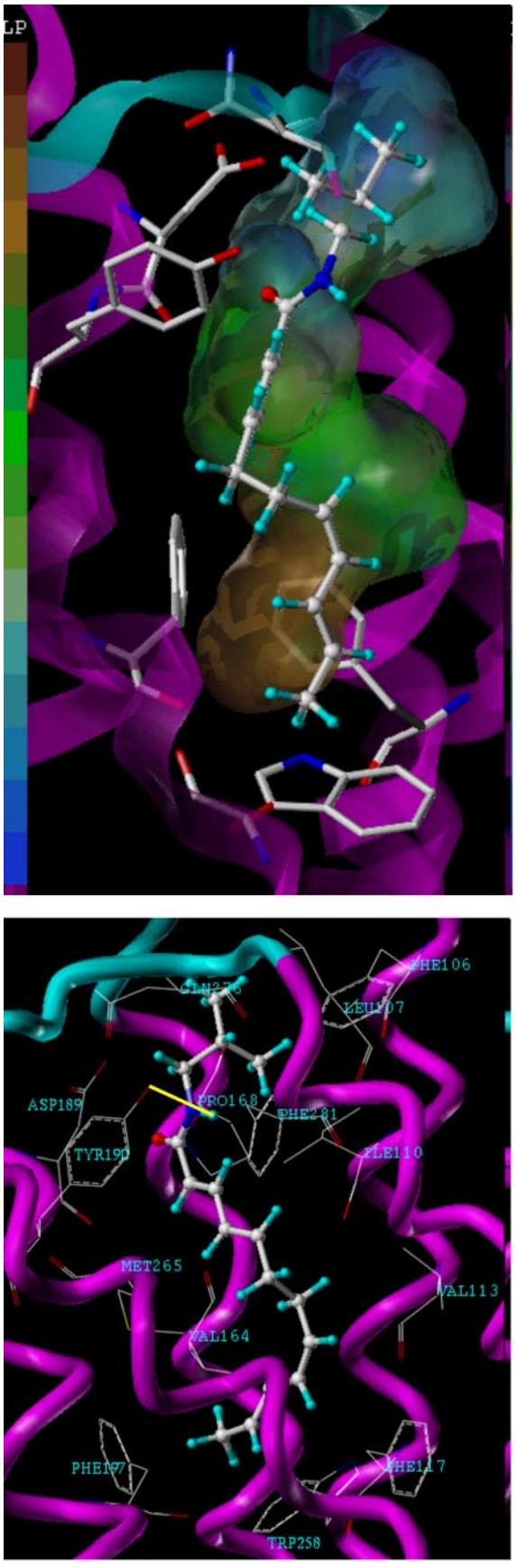

FIGURE 4. **Proposed binding conformation of alkylamides A1 and A2 in the CB_2 receptor.** *A,* putative binding site for CB_2 ligands is located adjacent to helices III, V, VI, and VII at the near extracellular side of the 7TM bundles. The surface is color-coded using the lipophilicity scale in which the hydrophilic center (*blue*) is framed by polar residues (*e.g.* Gln-276, Tyr-190, and Asp-189), and a hydrophobic cleft (*brown*) is surrounded by aromatic residues (*e.g.* Phe-197, Phe-117, and Trp-258). *B,* the putative interaction of alkylamides with the CB_2 receptor is shown. The oxygen atom in the hydroxyl group of Tyr-190 forms a hydrogen bond with the amide hydrogen of the alkylamide (shown by *yellow line* in *B*), and the aromatic ring of Tyr-190 exhibits π-π interactions with the C-2–C-3 double bond in the alkylamide.

relevant receptors but not CB_2. The corresponding data for CB_2 were obtained in our in-house assay using the same experimental conditions. Fig. 3 shows the % binding inhibition of the appropriate radioligands by A1 and A2 (single measurements), indicating that the compounds do not significantly interact with radioligand-binding sites on receptors other than the cannabinoid receptors in the screen. However, both compounds showed a tendency to also compete with radioligands specific to serotonin 2A and serotonin 2C receptors. In addition, A2 tends to compete with radioligands for norepinephrine transporter and the opioid κ receptor (Fig. 3). A1 did not significantly bind to the CB_1 receptor although A2 did, thus confirming the results of the independently conducted binding experiments (see above).

Molecular Modeling—The interaction of alkylamides with the CB_2 receptor was further explored in a homology model (25). The amphipathic cavity of the CB_2 model is approximately bound by the solvent-accessible surface as shown in Fig. 4*A*. A putative binding site for CB_2 ligands is located adjacent to helices III, V, VI, and VII at the near extracellular side of the 7TM bundles. The surface is color-coded using the lipophilicity scale in which the hydrophilic center (*blue*) is framed by polar residues (*e.g.* Gln-276, Tyr-190, and Asp-189), and a hydrophobic cleft (*brown*) is surrounded by aromatic residues (*e.g.* Phe-197, Phe-117, and Trp-258) (Fig. 4*A*). A recent review by Raitio *et al.* (32) has summarized the specific amino acid residues suggested to be important for CB_2 ligand activity. These include the residues Asp-130, Arg-131, Tyr-132 (33), Cys-174, and Cys-175, which are important for the conformation of the wild-type CB_2 receptor (34), and the residues Ser-161 and Ser-165, which are required for binding of the antagonist SR144528 (35), The residues Tyr-190 and Phe-197 have been shown to be necessary for the binding of agonists (36, 37). The distance between the hydrophilic and hydrophobic centers is estimated as 9–11 Å, which is a typical size of a cannabinoid ligand molecule. The alkylamide molecule A1 was initially docked into the putative binding region as shown in Fig. 4*A*, spanning the hydrophobic to hydrophilic regions and indicating the amphiphilic nature of isobutylamide-type alkylamides.

Like the putative cavity of the CB_2 model, alkylamides A1 and A2 are also amphipathic molecules with hydrophilic amide and hydrophobic alkyl groups, and their flexible molecular features allowed them to be docked well into the predicted binding pocket. The A1-CB_2 complex was then optimized by the Flexidocking and MD/MM simulations. The computer modeling indicated that the alkylamide molecule interacts with the CB_2 receptor (Fig. 4*B*). The amide group of the alkylamide is headed into the hydrophilic pocket, surrounded by the residues Asp-189 and Tyr-190 of the CB_2 receptor. The important residue Tyr-190 not only exhibits an H-bond interaction but also π-π interactions with the alkylamide (Fig. 4*B*). In these interactions, oxygen in the hydroxyl group of Tyr-190 forms a hydrogen bond with the amide hydrogen of the alkylamide (shown by *yellow line* in Fig. 4*B*), and the aromatic ring of Tyr-190 exhibits π-π interactions with the C-2–C-3 double bond in the alkylamide.

Alkylamides Elevate $[Ca^{2+}]_i$ in HL60 Cells via CB_2—We have shown previously that alkylamides influence cellular cAMP levels in monocytes/Mϕs and that they inhibit forskolin-induced cAMP formation (7). In this study, the CB_2-mediated effect on total $[Ca^{2+}]_i$ was assessed. We employed CB_2-positive and CB_2-negative cell lines (Fig. 5*A*) and first

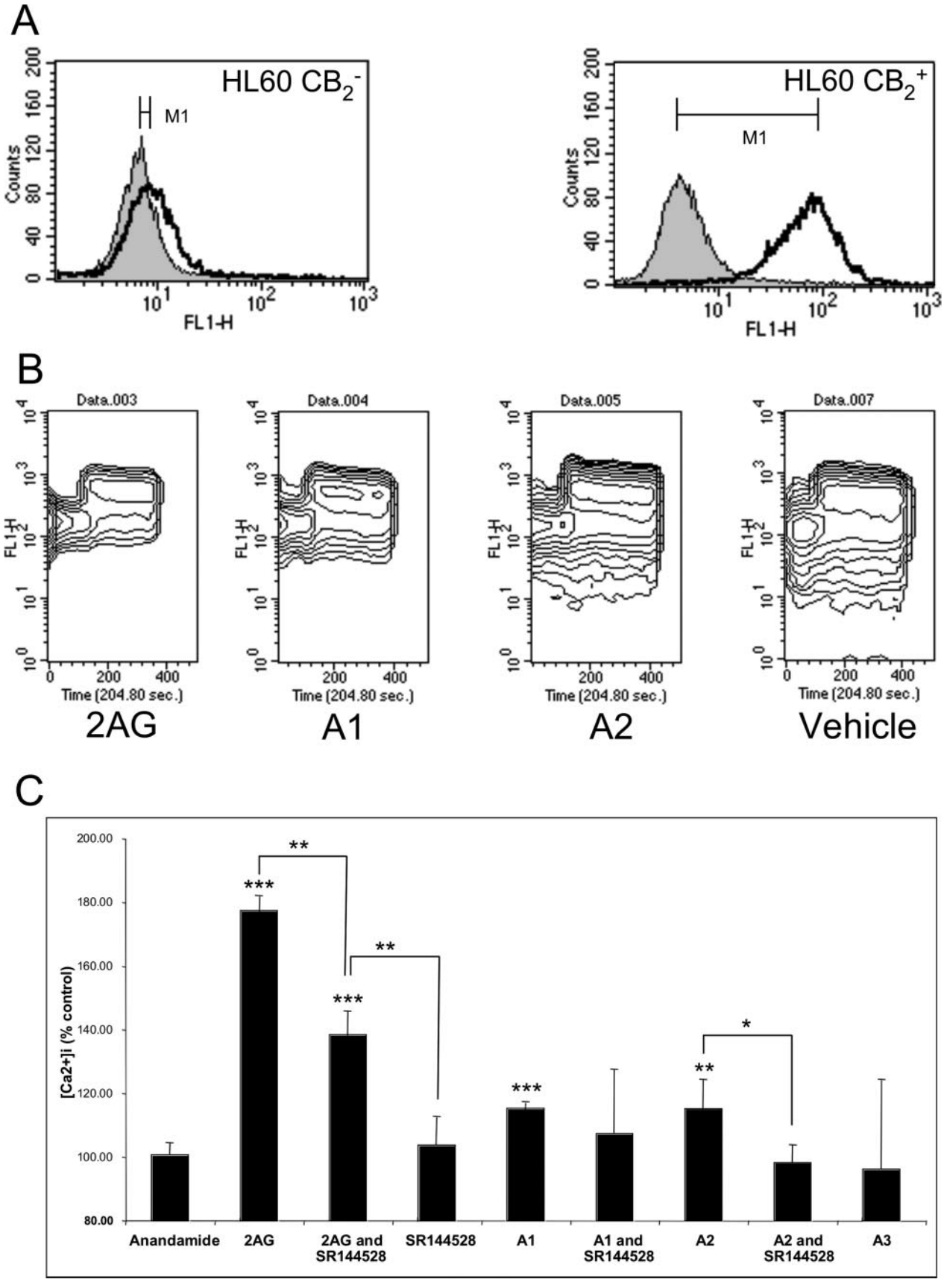

FIGURE 5. **The effects of alkylamides, anandamide, and 2-AG on $[Ca^{2+}]_i$ in HL60 cells.** The CB_2 receptor surface expression on HL60-negative (1) and -positive (2) cells was determined by FACS using the antibody 3561 (representative image of three independent experiments) (*A*). FACS density plot of total $[Ca^{2+}]_i$ in CB_2-positive HL60 cells over time was determined by fluo3/AM staining (*B*). 2-AG, A1, and A2 (10 μM each) elevated total $[Ca^{2+}]_i$(*C*). Addition of SR144528 (1 μM) partially inhibited the effect. Anandamide and A3 did not significantly influence $[Ca^{2+}]_i$. $n = 3 \pm$ S.D. *, $p = \leq 0.05$; **, $p = \leq 0.01$; ***, $p = \leq 0.001$.

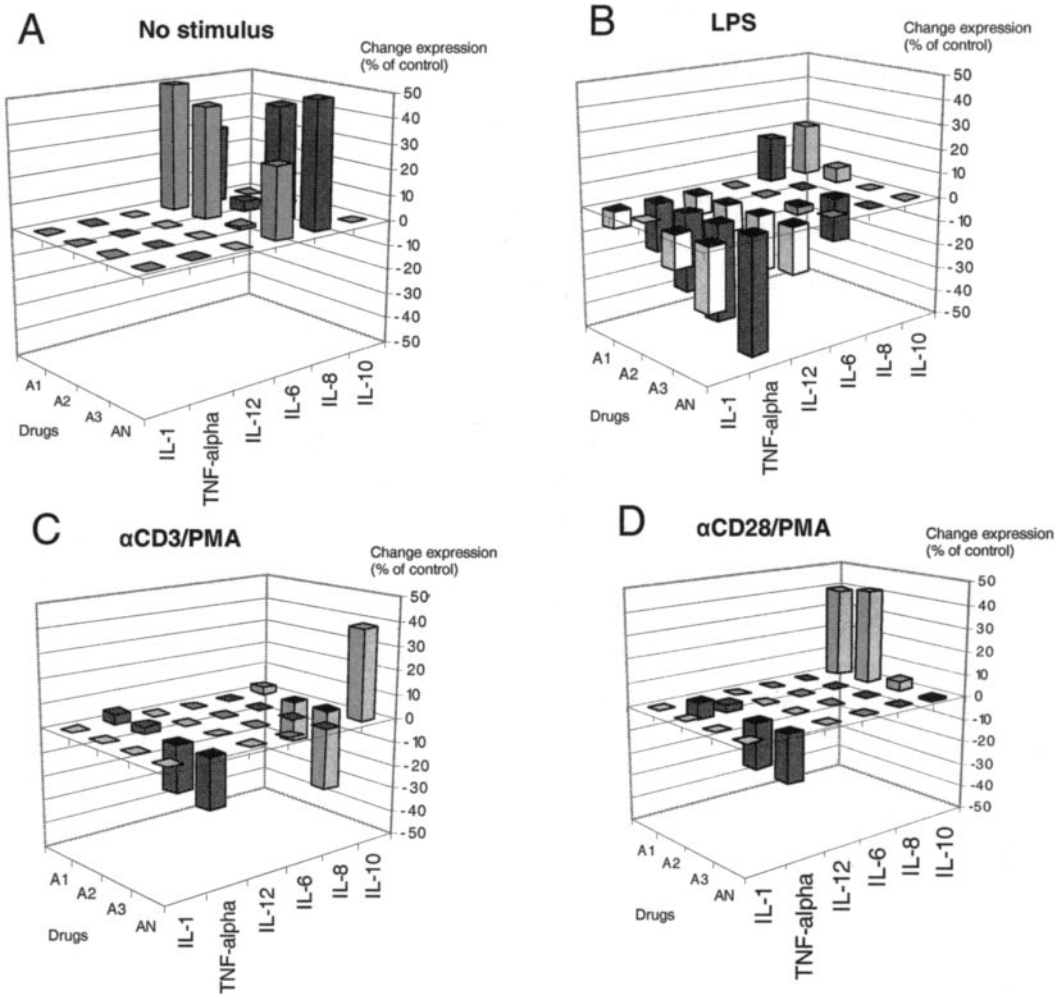

FIGURE 6. **Overview of immunomodulatory effects of alkylamides and anandamide using different stimuli.** 50 nM of drugs were incubated with CD3/PMA-stimulated, CD28/PMA-stimulated, nonstimulated, and LPS-stimulated whole blood for 18 h (see "Experimental Procedures"). Cytokines were quantified by FACS using CBAs. Anandamide (*AN*) and alkylamides from *Echinacea* (*A1–A3*) differentially modulate cytokine expression (% of stimulated control). Data are mean values ($n = 3$).

tested their sensitivity to thapsigargin. Measurements of the Ca^{2+} sensing dye fluo3/AM were performed real time in Ca^{2+}-free buffer by FACS (Fig. 5*B*). Thapsigargin, which promotes the discharge of Ca^{2+} from intracellular stores by specifically inhibiting endoplasmic reticulum Ca^{2+}-ATPase (38), led to an increase in total $[Ca^{2+}]_i$ in both cell lines (not shown). We could also confirm that 2-AG but not anandamide elevates $[Ca^{2+}]_i$ in HL60 cells, as was reported previously by Sugiura *et al.* (39) (Fig. 5*C*). 2-AG led to a significant increase (180% of vehicle control) in total $[Ca^{2+}]_i$ in CB_2-positive HL60 cells, which was suppressed by the CB_2 antagonist SR144528 (Fig. 5*C*). In these cells also A1 and A2 but not A3 significantly induced $[Ca^{2+}]_i$ elevation, and the effects could be inhibited by SR144528 (Fig. 5*C*). No significant modulation of $[Ca^{2+}]_i$ was detected in CB_2-negative HL60 cells (not shown), which clearly suggests that CB_2 is directly involved in Ca^{2+} signaling by 2AG, A1, and A2.

Effects on Constitutive Cytokine/Chemokine Expression in Human Whole Blood and HL60 Cells—In a next step we studied the effects of different concentrations of alkylamides A1, A2, and A3, anandamide, and SR144528 on constitutive cytokine/chemokine expression in human whole blood. The constitutive expression of pro-inflammatory proteins (TNF-α, IL-1β, and IL-6) was generally low (<30 pg/ml), and only the protein level of the chemokine IL-8 (CXCL8) was typically high (>100 pg/ml). First, the compounds were tested on constitutive (nonstimulated) whole blood. At low concentrations (<100 nM) SR144528 significantly inhibited IL-1β production, reducing constitutive expression to 75% of vehicle control (see the supplemental material). No effect on IL-1β expression was observed for any of the other compounds investigated. In contrast, the prominent constitutive expression of IL-8 was modulated by A1, A3, and anandamide (Fig. 6*A*). IL-8 was significantly up-regulated at low nanomolar concentrations (Fig. 6*A* and supplemental material). In order to test whether the modulation of IL-8 was related to interactions with the CB_2 receptor in myeloid cells, we carried out experiments with CB_2-positive and CB_2-negative HL60 cells, both of which constitutively express IL-8 protein. Our results show that in CB_2-positive HL60 cells, the constitutive IL-8 expression (249 ± 151 pg/ml) was either not affected (A1 and A3) or up-regulated (A2 and anandamide), whereas in CB_2-negative HL60 cells, IL-8 expression (620 ± 191 pg/ml) was inhibited by all compounds (see the supplemental material). Most interestingly, the CB_2 antagonist SR144528 inhibited IL-8 expression in both CB_2-positive and -negative HL60 cells (see the supplemental material).

Compounds A1, A2, and anandamide, but not A3, significantly up-regulated IL-6 protein expression to 130–160% of control levels in human whole blood (Figs. 6*A* and 7). Somewhat surprisingly, anandamide and A2 inhibited IL-6 at a concentration of 500 nM, thus showing a biphasic (bell-shaped) effect (Fig. 7). Because the non-CB_2-binding al-

kylamide A3 did not up-regulate IL-6 protein expression, the induction of IL-6 by A1, A2, and anandamide appears to be CB_2-dependent. This assumption is supported by the fact that the CB_2 antagonist SR144528 (500 nM) was able to inhibit the up-regulation of IL-6 (Fig. 7), which clearly suggests involvement of CB_2 in the modulation of IL-6 by A1, A2, and anandamide.

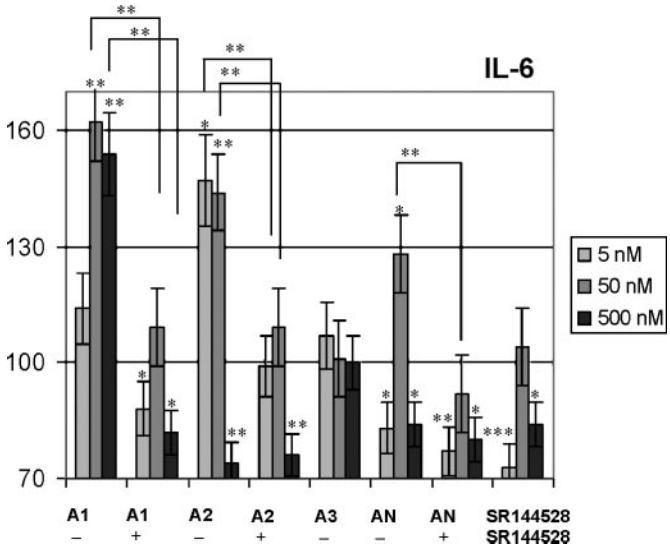

FIGURE 7. **The effects of alkylamides, anandamide, and SR144528 on constitutive IL-6 expression in human whole blood.** Drugs were incubated with nonstimulated whole blood for 18 h. Cytokines were quantified by CBAs. At 5 and 50 nM, all CB_2 agonists (determined by binding affinity to CB_2, effect on $[Ca^{2+}]_i$, or previously published effect on cAMP) significantly increased IL-6 levels in whole blood. The up-regulation was not seen with A3. The CB_2 antagonist SR144528 (1 μM) significantly inhibited the effect on IL-6 ($n = 6 \pm$ S.E., at least two different blood donors). *, $p = \leq 0.05$; **, $p = \leq 0.01$; ***, $p = \leq 0.001$.

Effects on Stimulated Cytokine/Chemokine Expression in Human Whole Blood—To further explore the immunomodulatory actions exerted by alkylamides from *Echinacea*, anandamide, and SR144528, human whole blood from healthy volunteers was stimulated with either LPS, αCD28/PMA, or αCD3/PMA (see "Experimental Procedures"). These stimuli trigger different signals and result in distinct cytokine expression patterns. LPS primarily induces IL-1, TNFα, IL-6, IL-8, and IL-10 expression from monocytes/Mϕs via CD14 and TLR-4 (40). CD28 signals via protein kinase C and protein-tyrosine kinases and promotes a TH_2 response (41), although CD3 stimulation results in the production of phospholipase Cγ, release of diacylglycerol, and the release of Ca^{2+} from intracellular stores, resulting in up-regulation of TH_1 and TH_2 cytokines (42) (see also Fig. 8). Therefore, by studying the changes in these distinct expression patterns in response to compound treatment, the actions of the different compounds on cytokine expression can be dissected, at least partially.

At low nanomolar concentrations A1, A2, A3, anandamide, and the CB_2 antagonist SR144528 all inhibited LPS-induced TNF-α, IL-1β, and IL12p70 expression (Figs. 6*B* and 9, *A–C*). As this was also the case for A3, the inhibition of LPS-triggered cytokine release is most likely not related to CB_2 binding. In contrast, the CB_2 receptor antagonist AM630 did not significantly inhibit TNF-α expression at low nanomolar concentrations but up-regulated TNF-α expression at 5000 nM by ~25% (Fig. 9*A*). Moreover, preliminary data show that the CB_2 antagonist AM630 (1 μM) can reverse the action of anand-

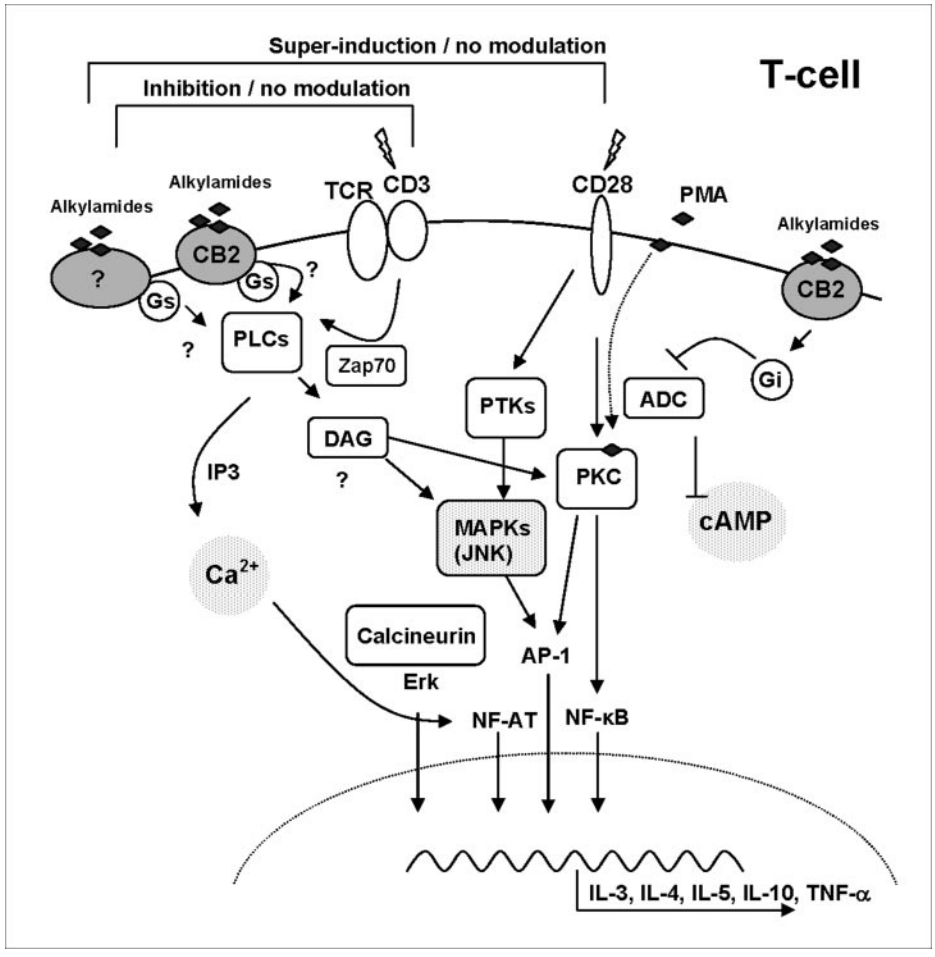

FIGURE 8. **Alkylamides co-stimulate CD28-activated cytokine expression and negatively regulate CD3/T-cell receptor.** CD28 signals via protein kinase C (*PKC*) and protein-tyrosine kinases (*PTKs*), leading to activation of transcription factors NF-κB and AP-1 (activating protein-1 (*AP-1*)). CD3 signals via PLCγ and activates inositol 3-phosphate (*IP3*), calcium, and diacylglycerol (*DAG*), leading to activation of the transcription factors nuclear factor of activated T-cells (*NF-AT*), NF-κB, and extracellular signal-related protein kinase (*Erk*). Alkylamides interact with CB_2 receptors and most likely another receptor, leading to an increase in total $[Ca^{2+}]_i$ (preliminary data), and activation of mitogen-activated kinases (*MAPKs*) (7). CD28 activation and co-stimulation with alkylamides leads to a significant super-induction (~150%) of IL-3 and IL-10. On the other hand, CD3 activation and co-stimulation with alkylamides leads to a significant inhibition (~20–50%) of IL-3, IL-5, and IL-10, thus suggesting that alkylamides can negatively regulate the CD3/T-cell receptor activation pathway.

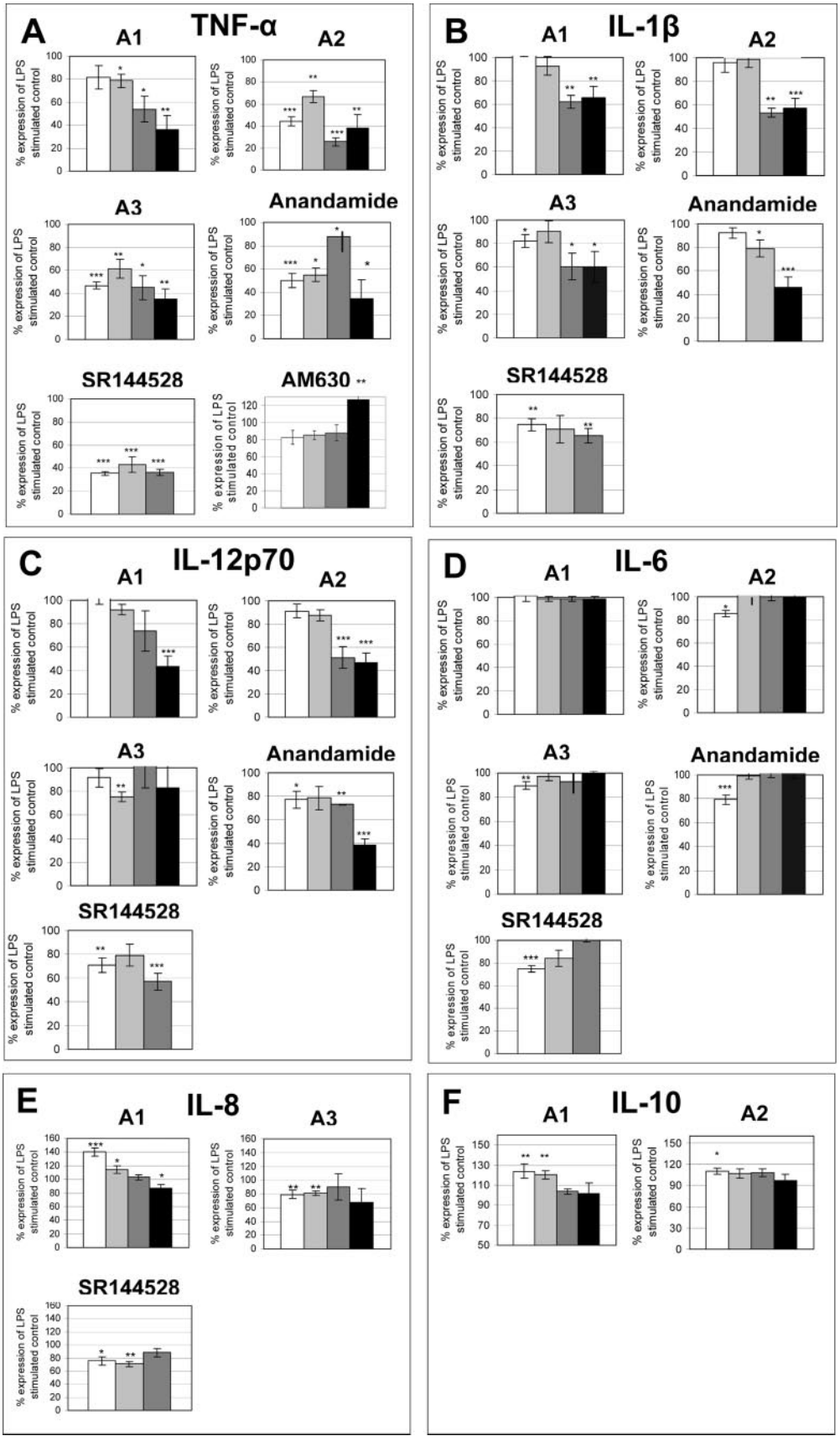

FIGURE 9. **Effects of alkylamides, anandamide, SR144528, and AM630 on LPS-stimulated cytokine expression in human whole blood.** Drugs were incubated for 1 h prior to LPS stimulation (313 ng/ml *E. coli*, 055:B3 LPS) of whole blood for 18 h at 5 nM (*white*), 50 nM (*light gray*), 500 nM (*dark gray*), and 5000 nM (*black*). Cytokines were quantified by CBAs. The alkylamides A1, A2, and A3 and also anandamide and the CB_2 antagonist SR144528 differentially inhibit LPS-induced cytokine expression. Only cytokines are shown where significant effects could be observed. Data from at least nine measurements derived from three different blood donors are shown (±S.E.). *, $p = \leq 0.05$; **, $p = \leq 0.01$; ***, $p = \leq 0.001$.

TABLE 2

Differential expression of cytokines after LPS, αCD3/PMA, and αCD28/PMA stimulation (see "Experimental Procedures") of human whole blood

Experiments were performed in triplicate with blood from at least three independent donors. Data are mean values ± S.D. Δp shows significant differences between αCD3- and αCD28-induced cytokine expressions. *, $p = \leq 0.05$; **, $p = \leq 0.01$; ***, $p = \leq 0.001$.

Cytokine	LPS	αCD3/PMA	αCD28/PMA	Δp	PMA only
	pg/ml	*pg/ml*	*pg/ml*		*pg/ml*
TNF-α	4266 ± 3202	2774 ± 533	4554 ± 469	***	978 ± 672
IL-1β	3905 ± 3763	1144 ± 1362	437 ± 403		172 ± 113
IL-6	2695 ± 1904	722 ± 479	398 ± 567		310 ± 269
IL-12p70	98 ± 56	84 ± 69	59 ± 47		<20
IL-10	2863 ± 1325	113 ± 31	72 ± 48	*	<20
IL-8	8571 ± 4648	5308 ± 236	4693 ± 485	**	2300 ± 951
GM-CSF	<20	750 ± 364	1324 ± 639	*	319 ± 205
IL-7	31 ± 27	74 ± 33	55 ± 30		52 ± 20
IL-5	<20	309 ± 19	392 ± 159		40 ± 13
IL-4	<20	54 ± 14	41 ± 12		23 ± 8
IL-3	<20	157 ± 63	61 ± 43	*	<20

amide on LPS-induced TNF-α in Mϕ-enriched mononuclear cells (see the supplemental material).

LPS-stimulated IL-6 was weakly inhibited at the lowest concentration (5 nM) by all compounds except for A1 (Fig. 9*D*). Moreover, A1 significantly up-regulated LPS-stimulated IL-8 (~140%) and IL-10 (~120%), but A3 and the CB_2 antagonist SR144528 significantly down-regulated IL-8 (~80%) (Fig. 9, *E* and *F*).

In T-cell stimulation, using a combination of αCD3 and αCD28 as the stimulus, the resulting strong cytokine expression is derived from a combination of cellular signaling pathways (Fig. 8), and modulation of an αCD3/αCD28-induced response provides only limited insight into pathway specificity. Experiments with human whole blood from different donors show that αCD3/PMA stimulation alone results in a distinct cytokine expression pattern from αCD28/PMA stimulation (Table 2). αCD28/PMA induces significantly more TNF-α and GM-CSF but less IL-3 and IL-8 than αCD3 (Table 2). These expression patterns were obtained reproducibly in whole blood from different blood donors (Table 2). Regarding the modulation of αCD28- and αCD3-stimulated cytokine expression, all three alkylamides from *Echinacea*, and partially also anandamide, showed a similar modulation pattern. Although αCD28/PMA-stimulated cytokines (IL-3, IL-4, IL-5, and IL-10) were either not modulated (IL-4 and IL-5) or super-induced (IL-3 and IL-10), αCD3/PMA-stimulated cytokines were not modulated (IL-4 and IL-10) or inhibited (IL-5 and IL-3) (Fig. 10, *B–D*). All compounds inhibited αCD3- but not αCD28-induced IL-3 (produced by both TH_1 and TH_2 cells) (Fig. 10*B*). This finding suggests that protein kinase C and protein-tyrosine kinase signaling mediated by αCD28 stimulation of T-cells in whole blood is either directly or indirectly co-stimulated by the alkylamides and partially also by anandamide (Fig. 8). On the other hand, αCD3-induced signaling via PLCγ is not influenced or inhibited (IL-3, IL-5, and IL-10) (Fig. 10, *B–D*).

The broad inhibitory effects by alkylamides and anandamide on LPS-stimulated TNF-α, IL-1β, and IL12p70 (Fig. 9) was neither visible with αCD3 nor αCD28 stimulation (Fig. 10*A*). Nevertheless, A2, A3, anandamide, and SR144528 weakly but significantly inhibited TNF-α expression at 50 nM by ~20% (Fig. 6, *C* and *D*, and Fig. 10*A*).

DISCUSSION

The results presented in this study demonstrate for the first time that certain isobutylamide-type alkylamides, which are the prominent lipid-like compounds in *Echinacea*, bind to the human CB_2 receptor with low nanomolar K_i values. The alkylamides A1 and A2 also show some affinity to the CB_1 receptor (Table 1) but at 30–100 times higher concentrations ($K_i > 1500$ nM). The total loss of binding to CB_2 observed with A3 (Table 1) and the theoretical binding conformation of A1 obtained in the CB_2 homology model (Fig. 4) suggest that these compounds need to adopt an extended pseudo-helical conformation for binding, as has been proposed for anandamide (43). In contrast, the docking study by McAllister *et al.* (44) suggests that anandamide needs to adopt a curved/U-shaped conformation to interact with the CB_1 receptor.

Although alkylamides are structurally similar to the endogenous cannabinoid anandamide, the anandamide molecule, containing an acyl chain with four nonconjugated double bonds, is more flexible than A1. Our current docking simulation studies indicate that alkylamides A1 and A2 fit into the putative binding pocket of the CB_2 receptor (Fig. 4*B*) with the alkyl tail located in the hydrophobic pocket formed by the aromatic side chains of Trp-258, Phe-197, Phe-117, and Tyr-190. In this binding arrangement, the double bond between C-2 and C-4 of the hydrocarbon would be involved in a favorable π-π interaction with the aromatic ring of Tyr-190. Such interactions are different from those expected for anandamide, which lacks the C-2–C-4 double bond. Our preliminary computer modeling studies reveal a possible CB_2 binding conformation of alkylamides highlighting the importance of Tyr-190. Currently, more systematic structure-activity relationship investigations of alkylamide analogs and CB_2 receptor ligand docking studies with anandamide are underway, and the results will be reported elsewhere.

Based on the observation that alkylamides exhibit surfactant behavior[3] and the partial lack of a concentration dependence of the effects observed in the displacement studies and biological assays, we believe that alkylamides may form micellar structures. Measurements of the critical micelle concentrations of alkylamides are in progress. A recently published study on the affinity of alkylamides from *E. angustifolia* to rodent cannabinoid receptors provided K_i values in the lower micromolar range (8), but in this study the displacement curve was not shown, and the solubility of alkylamides, which appears to be of key importance, was not discussed. Therefore, the discrepancy between the K_i values reported could either be due to structural differences between rodent and human CB_2 receptors, experimental conditions used, or even the interpretation of displacement curves.

Our results show that the CB_2-binding alkylamides A1 and A2 elevate total $[Ca^{2+}]_i$ in CB_2-positive but not in CB_2-negative promyelocytic HL60 cells (Fig. 5). Because this effect was clearly inhibited by the CB_2 antagonist SR144528, the response might be directly induced via a CB_2-mediated G-protein-coupled mechanism, leading to stimulation of PLC, a pathway known to be activated by CB_1 agonists (45). It has been

[3] S. Raduner and J. Gertsch, unpublished data.

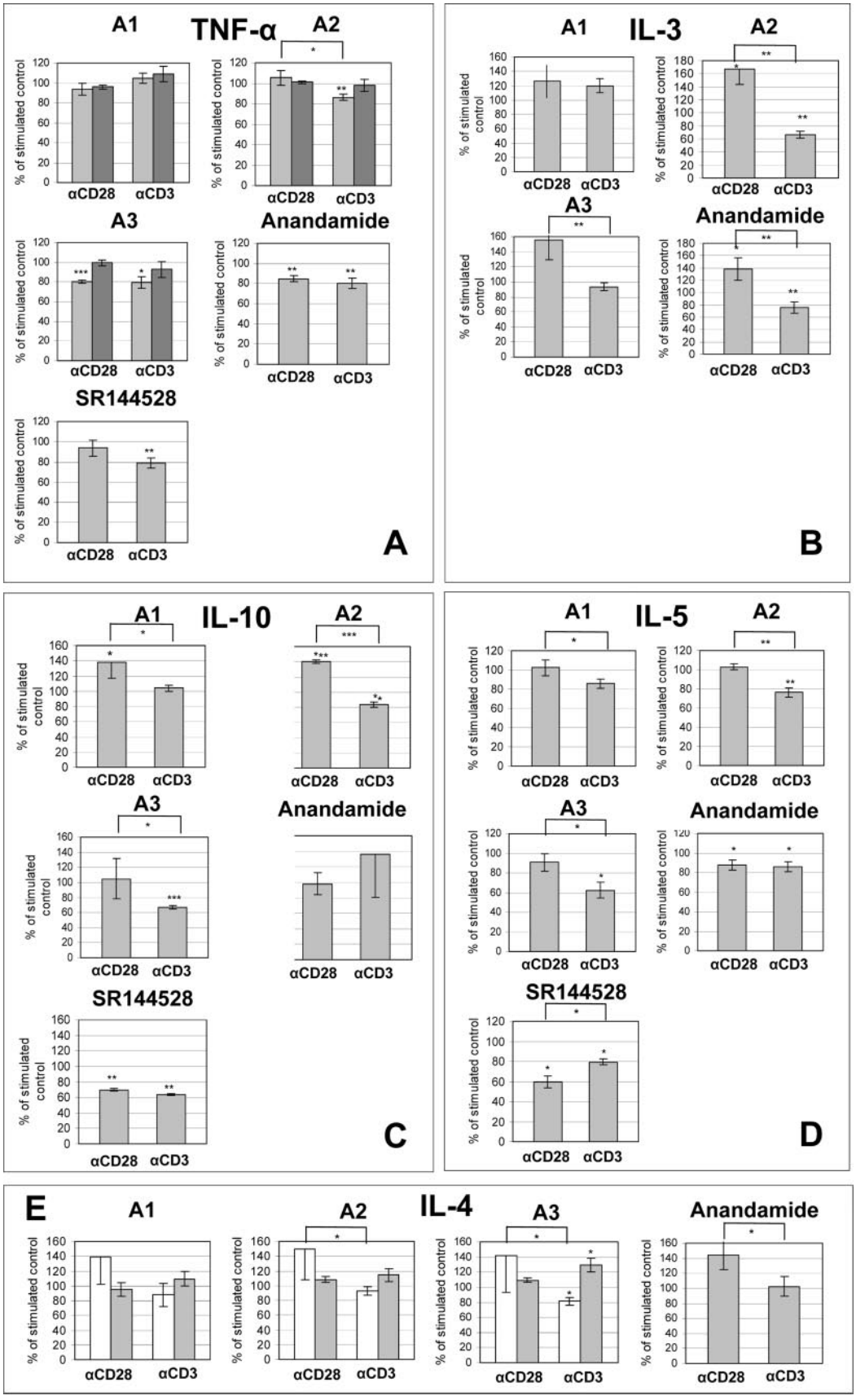

FIGURE 10. **The effects of alkylamides, anandamide, and SR144528 on αCD3- and αCD28-stimulated cytokine expression in human whole blood.** Only those cytokines are shown for which significant effects could be observed. Drugs were incubated with stimulated (1.5 μg/ml PMA; 1.0 μg/ml αCD3; 0.5 μg/ml αCD28) whole blood for 18 h with 5 nM (*white bars*) and 50 nM (*light gray bars*) of drugs. Cytokines were quantified by CBAs. Data from at least nine measurements derived from three different blood donors are shown (±S.E.). *, $p = \leq 0.05$; **, $p = \leq 0.01$; ***, $p = \leq 0.001$.

shown recently that Ca^{2+} transients stimulated by 2-AG in CB_2 receptor-transfected Chinese hamster ovary cells can be inhibited by the PLCβ inhibitor U73122 (46). The observation that 2-AG but not anandamide leads to a modulation of $[Ca^{2+}]_i$ in CB_2-positive HL60 cells is in agreement with previous data (39). Based on these data it has been suggested that 2-AG is the true CB_2 ligand. On the other hand, it has been postulated that anandamide binds first to the lipid bilayer and then moves into the receptor (47), implying a time-resolved diffusion. Because release of $[Ca^{2+}]_i$ occurs rapidly (<100 ms) and is measured in real time, it is possible that anandamide modulates $[Ca^{2+}]_i$ outside the time window normally chosen for such measurements. Preliminary data show that alkylamides from *Echinacea* also elevate total $[Ca^{2+}]_i$ in Jurkat T-cells (data not shown). The fact that Jurkat T-cells produce CB_2 mRNA (48), but exhibit only very low surface CB_2 protein expression,[3] may also suggest that a second receptor is involved in Ca^{2+} signaling for alkylamides but also 2-AG. This is also indicated by the fact that SR144528 is not able to fully inhibit $[Ca^{2+}]_i$ in HL60 cells induced by 2-AG and alkylamides (Fig. 5*C*).

It has been shown recently that Δ^9-tetrahydrocannabinol induces a Ca^{2+} influx in resting T-cells in a cannabinoid receptor-dependent manner (49). Together with the data presented in this study, the latter finding indicates that the known inhibitory effect on cAMP production mediated by CB_2 stimulation (50) is unlikely to represent the only mechanism underlying immune modulation by cannabinoids.

As cannabinoids (including the endogenous cannabinoids) have been reported to exert anti-inflammatory and immunosuppressive effects both *in vitro* and *in vivo* (18, 19), we also studied the actions of alkylamides A1 to A3, anandamide, and SR144528 on untreated and stimulated human whole blood. Overall, αCD3- and αCD28-stimulated whole blood showed both TH_1- and TH_2-type cytokine expressions, whereas LPS resulted in the characteristic expression of IL-1β, IL-6, IL-8, and TNF-α (Table 2). Interferon-γ expression was not measured. In our system (18-h incubation of undiluted heparinized whole blood), only IL-1β, IL-6, IL-7, and IL-8 were constitutively expressed (>20 pg/ml) under nonstimulating conditions.

The CB_2-binding compounds A1, A2, and anandamide significantly up-regulated constitutive IL-6 expression (Fig. 7). As the up-regulation of IL-6 in human whole blood cultures was strongly inhibited by SR144528, and the non-CB_2-binding compound A3 did not show an effect on constitutive IL-6, it is likely that the up-regulation of IL-6 expression is mediated via the CB_2 receptor. Moreover, SR144528 at 5 nM completely inhibited the weak constitutive IL-6 expression (Fig. 7), which may be the result of the inverse agonistic action. Anandamide has been shown previously to potentiate IL-6 expression in infected astrocytes, possibly via a cannabinoid receptor-dependent pathway (51). In a different study it was also shown that mice injected with 8 mg/kg Δ^9-tetrahydrocannabinol produced high levels of IL-6 (52). IL-6 is a pro-inflammatory cytokine, which is produced by professional antigen-presenting cells, such as B cells, Mϕs, and dendritic cells (53), and plays multiple pro-inflammatory but also anti-inflammatory roles in the cellular immune system (54). IL-6 activity appears to be critical for the effective management of acute inflammation and subsequent resolution, but it is also associated with chronic inflammatory diseases (54).

Anandamide and alkylamides A1 and A2 also showed modulatory effects on constitutive IL-8 expression (Fig. 6*A*). That cannabinoids modulate IL-8 expression has been reported previously (55, 56). The potent synthetic cannabinoid receptor agonist CP-55940 and the endocannabinoid 2-AG were shown to up-regulate IL-8 expression in HL60 cells at nanomolar (55) and micromolar (56) concentrations, respectively. In our experiments, alkylamides A1–A3, as well as anandamide, significantly up-regulated IL-8 expression (150–225%) in human whole blood at low nanomolar concentrations. In CB_2-negative HL60 cells constitutive IL-8 expression was inhibited or not influenced, whereas in CB_2-positive cells IL-8 was up-regulated by A2 and anandamide (see the supplemental material). The antagonist clearly inhibited constitutive IL-8 expression at 50 nM in both cell lines but not in whole blood (supplemental material). Because A3, which does not bind to CB_2, also showed a modulation of IL-8 (Fig. 6*A* and see the supplemental material), it seems likely that CB_2 interaction is not the primary underlying mechanism.

Overall, the compounds investigated in our study exert their most potent effects on the LPS-induced expression of monocyte/Mϕ cytokines TNF-α, IL-1β, and IL-12p70 (Figs. 6 and 9) and only weakly modulated the levels of αCD3/PMA- and αCD28/PMA-stimulated cytokines from T-cells (Fig. 10). The potent inhibitory action of anandamide on LPS-induced TNF-α (IC_{50} <5 nM) is likely to be independent of its reported inhibitory effect on NF-κB (57), because the latter was only observed at 1000 times higher concentrations. αCD3/PMA- and αCD28/PMA-stimulated TNF-α was inhibited less effectively (IC_{50} >50 nM), and IL-1β and IL-12p70 expression was not inhibited at all (Fig. 6). Moreover, the moderate inhibition (~20%) of TNF-α is likely to reflect inhibition of the PMA stimulus only (Table 2) and not inhibition of the CD3 and CD28 receptor-mediated signals. This clearly shows that anandamide and the alkylamides from *Echinacea* specifically inhibit the LPS-stimulated release of TNF-α, IL-1β, and IL-12p70 but not IL-6 and IL-8. The molecular mechanisms underlying these effects are currently investigated in our laboratory.

Alkylamides co-stimulate cytokines from αCD28/PMA- but not αCD3/PMA-stimulated whole blood, and they promote $[Ca^{2+}]_i$, which suggests involvement of PLC (Fig. 8). In αCD28/PMA-stimulated cytokine release PLC is not involved, and its likely stimulation by alkylamides may thus lead to a weak co-stimulation, resulting in super-expression of cytokines like IL-3, IL-4, and IL-10. Activation of PLC through the CB_2 receptor by anandamide has been shown in calf pulmonary endothelial cells (58). Further experiments will have to determine whether alkylamides but also endocannabinoids can activate PLC isotypes in immune cells.

It was recently shown that alkylamides from *Echinacea* are resorbed *in vivo* and can be detected in nanomolar concentrations (0.5–50 nM) in human blood plasma upon ingestion (26, 27).

Our study shows for the first time that alkylamides from *Echinacea*, as well as anandamide, influence the cytokine milieu in human whole blood at low nanomolar concentrations (Figs. 5–8). Moreover, alkylamides can exert both anti- but also pro-inflammatory effects in human blood, depending on the stimulus applied, drug concentration used, and degree of unsaturation of the lipophilic tail of the specific alkylamide. The latter is shown by the fact that A1 exerts significantly distinct effects from A2, as exemplified in the experiments with LPS-stimulated human whole blood (Fig. 9). Although 5 nM of A1 super-stimulated LPS-induced IL-8 (~140%) and IL-10 (~125%) expression, 5 nM of A2 had no effect on IL-8, and only weakly up-regulated IL-10 (~110%).

Interestingly, the non-CB_2-binding alkylamide A3 also inhibited the expression of LPS-induced cytokines (Fig. 9), which must occur through a cannabinoid receptor-independent mechanism. Therefore, the prominent anti-inflammatory action of alkylamides and anandamide (see below) at concentrations below the CB_2 receptor K_i values probably involves a cannabinoid receptor-independent high affinity target, which is likely to be common to alkylamides and possibly also to endogenous cannabinoids.

Anandamide is known to exert differential effects on cytokine expres-

sion in leukocytes (18), but many of the corresponding studies were carried out with concentrations in the micromolar range. Our data demonstrate that even low nanomolar concentrations suffice to produce significant effects on cytokine expression in human whole blood (Figs. 5–8). At 5 nM anandamide potently inhibits LPS-induced TNF-α expression (IC_{50} <5 nM) (Fig. 9) but has no effect on IL-10 and IL-8 (not shown). However, the concentrations at which these effects were observed with anandamide are clearly below its CB_2 receptor K_i value (218 ± 149) (Table 1), and it is difficult to rationalize these effects solely on the basis of a CB_2-dependent mechanism. These findings re-emphasize previous reports, which have suggested that (endo)cannabinoids possess immuno-modulatory properties, which are independent of their interaction with the cannabinoid receptors (59, 60). Nonetheless, preliminary data show that the CB_2 antagonist AM630 can reverse the inhibition on LPS-induced TNF-α expression in Mϕ-enriched cell cultures (see the supplemental material). Thus, more detailed studies on the differential effects of different CB_2 antagonists would be useful.

Although this was not the focus of our study, it is nonetheless noteworthy that the CB_2 antagonist SR144528 (5–50 nM) showed potent inhibitory effects on cytokine expression, which are difficult to explain by its antagonistic action on the CB_2 receptor. SR144528 weakly but significantly inhibited constitutive IL-1β expression (supplemental material). Moreover, its inhibitory action on LPS-stimulated TNF-α, IL-1β, IL12p70, IL-6, and IL-8 and also αCD3/αCD28-stimulated IL-5 and IL-10 shows that both pro-inflammatory TH_1 and also TH_2 cytokines are inhibited. At 5 nM SR144528 potently inhibits LPS-induced TNF-α (IC_{50} <5 nM) (Fig. 9) but has no effect on IL-10 expression (not shown), which is also strongly induced by LPS. On the contrary, AM630 did not show an inhibitory effect on LPS-induced TNF-α expression at concentrations below 1 μM (Fig. 9). The compound SR144528 has been described as an inverse CB_2 agonist (61), but it remains to be elucidated whether all of its immunomodulatory effects are related to CB_2 interactions. Independent of this, our data are in line with recently reported studies on the anti-inflammatory action of the CB_2-specific inverse agonist triaryl bis-sulfone Sch.336, which was shown to exert potent anti-inflammatory effects in a disease model for allergic asthma (62).

Our data demonstrate that alkylamides from *Echinacea* are a new class of CB_2-specific cannabinomimetics, which share the anti-inflammatory properties of anandamide and the cannabinoids from *Cannabis sativa* (19). With respect to the intracellular responses triggered via the CB_2 receptor, alkylamides from *Echinacea* resemble the endogenous cannabinoid 2-AG, which also stimulates Ca^{2+} transients in a CB_2 receptor-dependent manner (39, 46). The fact, however, that the anti-inflammatory effects exerted by cannabinomimetics are not strictly CB_2-dependent, as shown in this and previous studies (59, 60), raises the question about a possible common second target.

Echinacea preparations have been claimed to exert both stimulatory and inhibitory effects on immune cells (20–21). The evaluation of the immunomodulatory actions of alkylamides, which represent one of the most important constituent classes of *Echinacea*, thus constitutes an important step on the way to a better understanding of the molecular and pharmacological nature of these herbal remedies.

The finding that alkylamides from *Echinacea* bind to CB_2 with K_i values in a concentration range that is also achievable *in vivo* provides a first insight into a possible molecular mechanism of action of alkylamide-containing *Echinacea* preparations. With regard to the medical use of *Echinacea* preparations for the common cold, there is currently no evidence that alkylamides may have beneficial effects other than their likely anti-inflammatory action during acute inflammation as suggested by this study. Additional studies are required to investigate whether alkylamides and cannabinoids can modulate the immune response triggered during viral infections.

Acknowledgments—We gratefully acknowledge Sanofi Synthelabo for providing the noncommercial specific CB_2 antagonist SR144528 and Dr. Reg Lehmann, MediHerb, Brisbane, Australia, for generously providing the alkylamide references. We thank Dr. Michael Detheux from Euroscreen S.A., Belgium, for the CB_2-transfected CHO-K1 cell line; Prof. Dr. Verena Dirsch, University of Vienna, Austria, for the CB_2-negative HL60 cell line; and Bioforce AG, Switzerland, for kindly providing crude E. purpurea root material. S. R. thanks Prof. Dr. Jörg Heilmann for the initial financial support and encouragement to participate in science. We also thank all volunteer blood donors at Institute of Pharmaceutical Sciences, ETH Zürich, and MD Christian-Olaf Bader for the numerous expert blood collections.

REFERENCES

1. Goel, V., Lovlin, R., Barton, R., Lyon, M. R., Bauer, R., Lee, T. D., and Basu, T. K. (2004) *J. Clin. Pharmacol. Ther.* **29,** 75–83
2. Barnes, J., Anderson, L. A., Gibbons, S., and Phillipson, J. D. (2005) *J. Pharm. Pharmacol.* **57,** 929–954
3. Randolph, R. K., Gellenbeck, K., Stonebrook, K., Brovelli, E., Qian, Y., Bankaitis-Davis, D., and Cheronis, J. (2003) *Exp. Biol. Med.* **228,** 1051–1056
4. Turner, R. B., Bauer, R., Woelkart, K., Hulsey, T. C., and Gangemi, J. D. (2005) *N. Engl. J. Med.* **353,** 341–348
5. Brinkeborn, R. M., Shah, D. V., and Degenring, F. H. (1999) *Phytomedicine* **6,** 1–6
6. Percival, S. (2000) *Biochem. Pharmacol.* **60,** 155–158
7. Gertsch, J., Schoop, R., Kuenzle, U., and Suter, A. (2004) *FEBS Lett.* **577,** 563–569
8. Woelkart, K., Xu, W., Pei, Y., Makriyannis, A., Picone, R. P., and Bauer, R. (2005) *Planta Med.* **71,** 701–705
9. De Petrocellis, L., Cascio, M. G., and Di Marzo, V. (2004) *Br. J. Pharmacol.* **141,** 765–774
10. Munro, S., Thomas, K. L., and Abu Shaar, M. (1993) *Nature* **365,** 61–65
11. Galiegue, S., Mary, S., Marchand, J., Dussossoy, D., Carriere, D., Carayon, P., Bouaboula, M., Shire, D., Le Fur, G., and Casellas, P. (1995) *Eur. J. Biochem.* **232,** 54–61
12. Matias, I., Pochard, P., Orlando, P., Salzet, M., Pestel, J., and Di Marzo, V. (2002) *Eur. J. Biochem.* **269,** 3771–3778
13. Oka, S., Yanagimoto, S., Ikeda, S., Gokoh, M., Kishimoto, S., Waku, K., Ishima, Y., and Sugiura, T. (2005) *J. Biol. Chem.* **280,** 18488–18497
14. Quartilho, A., Mata, H. P., Ibrahim, M. M., Vanderah, T. W., Porreca, F., Makriyannis, A., and Malan, T. P., Jr. (2003) *Anesthesiology* **99,** 955–960
15. Carlisle, S. J., Marciano-Cabral, F., Staab, A., Ludwick, C., and Cabral, G. A. (2002) *Int. Immunopharmacol.* **2,** 69–82
16. Parolaro, D., Massi, P., Rubino, T., and Monti, E. (2002) *Chem. Phys. Lipids* **108,** 169–190
17. Klein, T. W. (2005) *Nat. Rev. Immunol.* **5,** 400–411
18. Klein, T. W., Newton, C., Larsen, K., Lu, L., Perkins, I., Nong, L., and Friedman, H. (2003) *J. Leukocyte Biol.* **74,** 486–496
19. Croxford, J. L., and Yamamura, T. (2005) *J. Neuroimmunol.* **166,** 3–18
20. Sarfaraz, S., Afaq, F., Adhami, V. M., and Mukhtar, H. (2005) *Cancer Res.* **65,** 1635–1641
21. Blazquez, C., Casanova, M. L., Planas, A., Del Pulgar, T. G., Villanueva, C., Fernandez-Acenero, M. J., Aragones, J., Huffman, J. W., Jorcano, J. L., and Guzman, M. (2003) *FASEB J.* **17,** 529–531
22. Steffens, S., Veillard, N. R., Arnaud, C., Pelli, G., Burger, F., Staub, C., Karsak, M., Zimmer, A., Frossard, J. L., and Mach, F. (2005) *Nature* **434,** 782–786
23. Devane, W. A., Dysarz, F. A., III, Johnson, M. R., Melvin, L. S., and Howlett, A. C. (1988) *Mol. Pharmacol.* **34,** 605–613
24. Kaminski, N. E., Abood, M. E., Kessler, F. K., Martin, B. R., and Schatz, A. R. (1992) *Mol. Pharmacol.* **42,** 736–742
25. Xie, X. Q., Chen, J. Z., and Billings, E. M. (2003) *Proteins* **53,** 307–319
26. Woelkart, K., Koidl, C., Grisold, A., Gangemi, J. D., Turner, R. B., Marth, E., and Bauer, R. (2005) *J. Clin. Pharmacol.* **45,** 683–689
27. Matthias, A., Addison, R. S., Penman, K. G., Dickinson, R. G., Bone, K. M., and Lehmann, R. P. (2005) *Life Sci.* **77,** 2018–2029
28. Calignano, A., La Rana, G., Giuffrida, A., and Piomelli, D. (1998) *Nature* **394,** 277–281
29. Cheng, Y. C., and Prusoff, W. H. (1973) *Biochem. Pharmacol.* **22,** 3099–3108
30. Palczewski, K., Kumasaka, T., Hori, T., Behnke, C. A., Motoshima, H., Fox, B. A., Le Trong, I., Teller, D. C., Okada, T., Stenkamp, R. E., Yamamoto, M., and Miyano, M. (2000) *Science* **289,** 739–745
31. Bauer, R., Reminger, P., and Wagner, H. (1988) *Phytochemistry* **27,** 2339–2342
32. Raitio, K. H., Salo, O. M., Nevalainen, T., Poso, A., and Jarvinen, T. (2005) *Curr. Med.*

Chem. **12,** 1217–1237
33. Feng, W., and Song, Z. H. (2003) *Biochem. Pharmacol.* **65,** 1077–1085
34. Shire, D., Calandra, B., Delpech, M., Dumont, X., Kaghad, M., Le Fur, G., Caput, D., and Ferrara, P. (1996) *J. Biol. Chem.* **271,** 6941–6946
35. Gouldson, P., Calandra, B., Legoux, P., Kerneis, A., Rinaldi-Carmona, M., Barth, F., Le Fur, G., Ferrara, P., and Shire, D. (2000) *Eur. J. Pharmacol.* **401,** 17–25
36. McAllister, S. D., Tao, Q., Barnett-Norris, J., Buehner, K., Hurst, D. P., Guarnieri, F., Reggio, P. H., Nowell Harmon, K. W., and Cabral, G. A. (2002) *Biochem. Pharmacol.* **63,** 2121–2136
37. Song, Z. H., Slowey, C.-A., Hurst, D. P., and Reggio, P. H. (1999) *Mol. Pharmacol.* **56,** 834–840
38. Sagara, Y., and Inesi, G. (1991) *J. Biol. Chem.* **266,** 13503–13506
39. Sugiura, T., Kondo, S., Kishimoto, S., Miyashita, T., Nakane, S., Kodaka, T., Suhara, Y., Takayama, H., and Waku, K. (2000) *J. Biol. Chem.* **275,** 605–612
40. Beutler, B., and Cerami, A. (1986) *Nature* **320,** 584–588
41. Skapenko, A., Lipsky, P. E., Kraetsch, H. G., Kalden, J. R., and Schulze-Koops, H. (2001) *J. Immunol.* **166,** 4283–4292
42. Dasgupta, J. D., Granja, C., Druker, B., Lin, L. L., Yunis, E. J., and Relias, V. (1992) *J. Exp. Med.* **175,** 285–288
43. Chen, J.-Z., Han, X.-W., and Xie, X.-Q. (2005) *Life Sci.* **76,** 2053–2069
44. McAllister, S. D., Rizvi, G., Anavi-Goffer, S., Hurst, D. P., Barnett-Norris, J., Lynch, D. L., Reggio, P. H., and Abood, M. E. (2003) *J. Med. Chem.* **46,** 5139–5152
45. Lograno, M. D., and Romano, M. R. (2004) *Eur. J. Pharmacol.* **494,** 55–62
46. Shoemaker, J. L., Ruckle, M. B., Mayeux, P. R., and Prather, P. L. (2005) *J. Pharmacol. Exp. Ther.* **315,** 828–838
47. Makriyannis, A., Tian, X., and Guo, J. (2005) *Prost. Lipid Med.* **77,** 210–218
48. Schatz, A. R., Lee, M., Condie, R. B., Pulaski, J. T., and Kaminski, N. E. (1997) *Toxicol. Appl. Pharmacol.* **142,** 278–287
49. Rao, G. K., Zhang, W., and Kaminski, N. E. (2004) *J. Leukocyte Biol.* **75,** 884–892
50. Demuth, D. G., and Molleman, A. (2005) *Life Sci.* **78,** 549–568
51. Molina-Holgado, F., Molina-Holgado, E., and Guaza, C. (1998) *FEBS Lett.* **433,** 139–142
52. Klein, T. W., Newton, C., Widen, R., and Friedman, H. (1993) *J. Pharmacol. Exp. Ther.* **267,** 635–640
53. Diehl, S., and Rincon, M. (2002) *Mol. Immunol.* **39,** 531–536
54. Jones, S. A. (2005) *J. Immunol.* **175,** 3463–3468
55. Jbilo, O., Derocq, J. M., Segui, M., Le Fur, G., and Casellas, P. (1999) *FEBS Lett.* **448,** 273–277
56. Kishimoto, S., Kobayashi, Y., Oka, S., Gokoh, M., Waku, K., and Sugiura, T. (2004) *J. Biochem.* (*Tokyo*) **135,** 517–524
57. Sancho, R., Calzado, M. A., Di Marzo, V., Appendino, G., and Munoz, E. (2003) *Mol. Pharmacol.* **63,** 429–438
58. Zoratti, C., Kipmen-Korgun, D., Osibow, K., Malli, R., and Graier, W. F. (2003) *Br. J. Pharmacol.* **140,** 1351–1362
59. Kaplan, B. L., Rockwell, C. E., and Kaminski, N. E. (2003) *J. Pharmacol. Exp. Ther.* **306,** 1077–1085
60. Kaplan, B. L., Ouyang, Y., Rockwell, C. E., Rao, G. K., and Kaminski, N. E. (2005) *J. Leukocyte Biol.* **77,** 966–974
61. Rhee, M. H., and Kim, S. K. J. (2002) *Vet. Sci.* **3,** 179–184
62. Lunn, C. A., Fine, J. S., Rojas-Triana, A., Jackson, J. V., Fan, X., Kung, T. T., Gonsiorek, W., Schwarz, M. A., Lavey, B., Kozlowski, J. A., Narula, S. K., Lundell, D. J., Hipkin, R. W., and Bober, L. A. J. (2005) *Pharmacol. Exp. Ther.* **316,** 780–788
63. Showalter, V. M., Compton, D. R., and Abood, M. E. (1996) *J. Pharmacol. Exp. Ther.* **278**, 989–999
64. Mechoulam, R., Ben-Shabat, S., Hanus, L., Ligumsky, M., Kaminski, N. E., Schatz, A. R., Gopher, A., Almog, S., Martin, B. R., Compton, D. R., Pertwee, R. G., Griffin, G., Bayewitch, M., Barg, J., and Vogel, Z. (1995) *Biochem. Pharmacol.* **50**, 83–90
65. Rinaldi-Carmona, M., Barth, F., Millan, J., Derocq, J.-M., Casellas, P., Congy, C., Oustric, D., Sarran, M., Bouaboula, M., Calandra, M. P., shire, C., Brelière, J.-C., and Le Fur, G. l. (1998) *J. Pharmacol. Exp. Ther.* **284**, 644–650